

## REVERSE ENGINEERING AND FINITE ELEMENT ANALYSIS OF Ti-6Al-4V ORTHOPAEDIC HIP IMPLANTS


### REVERZNI INŽENJERING I ANALIZE METODOM KONAČNIH ELEMENATA VEŠTAČKIH KUKOVA OD Ti-6Al-4V LEGURE





Originalni naučni rad / Original scientific paper

Rad primljen / Paper received: 17.10.2024

<https://doi.org/10.69644/ivk-2024-03-0269>

Adresa autora / Author's address:

<sup>1)</sup> Innovation Centre of the Faculty of Mechanical Engineering, Belgrade, Serbia \*email: [kbojic@mas.bg.ac.rs](mailto:kbojic@mas.bg.ac.rs) K. Čolić  0000-

0002-0227-0026; S. Sedmak  0000-0002-2674-541X; I. Filipović  0000-0002-7977-2980; A. Milovanović  0000-0003-4668-8800; T. Smoljanić  0000-0002-0641-3223; F. Vučetić  0000-0002-7194-4880

<sup>2)</sup> 'Victor Babes' University of Medicine and Pharmacy, Dept. of Internal Medicine, Timisoara, Romania

#### Keywords

- partial hip implant
- finite element method
- Ti-6Al-4V alloy
- 3D scanning

#### Abstract

The goal of the research presented is to combine reverse engineering methodologies with a numerical approach to analyse the structural integrity of artificial hip implants made of Ti-6Al-4V alloy subjected to different types of loads. In this way, numerical models validate the adopted methodology for obtaining implant geometry using 3D scanning, while also providing valuable insight into the behaviour of hip implants under different static loading cases. Since 3D scanning is proven as efficient and reliable for obtaining accurate geometry of various types of implants, it is applied in this research. Following a detailed development of a hip implant model geometry, involving 3D scanning and refining the obtained point cloud to a level that would realistically represent the actual hip implant, numerical models are made based on the obtained geometry. Results of these simulations using the finite element method in ANSYS<sup>®</sup> software have provided realistic values of stresses in most critical areas of the hip implant. The precise value of load that would produce plastic strain on the implant is also determined and is used as the limit criterion for selecting load cases for further analysis. This analysis would involve the assessment of fatigue life of hip implants with the same geometry and the same material while assuming the presence of a crack in the most critical area.

#### INTRODUCTION

FEM is increasingly used to analyse the stress state of bones and prostheses, as well as fracture fixation devices. When it comes to the field of orthopaedics, there has always been a great interest in defining the acting stresses and loads in joints and prostheses /1-5/. However, the mathematical tools available for stress analysis in classical mechanics were not suitable for the calculation of highly irregular structural features of bones and implants. Therefore, the use of FEM was a logical step due to its unique ability to determine the stress state of structures with complex geometries, loading, and behaviour of biomaterials, /6-8/.

Although this method is approximate, but common in biomedicine due to the difficulty of obtaining an exact solution

#### Ključne reči

- parcijalni veštački kuk
- metoda konačnih elemenata
- Ti-6Al-4V legura
- 3D skeniranje

#### Izvod

Cilj istraživanja u ovom radu je kombinovanje metodologije reverznog inženjeringa sa numeričkim pristupom kako bi se uradila analiza integriteta implantata veštačkog kuka od legure Ti-6Al-4V, izloženih različitim vrstama opterećenja. Na taj način bi numerički modeli potvrdili usvojenu metodologiju za dobijanje geometrije implantata korišćenjem 3D skeniranja, a istovremeno bi pružili dragocen uvid u ponašanje implantata kuka u različitim slučajevima statičkog opterećenja. Pošto se 3D skeniranje pokazalo kao efikasno i pouzdano metod za dobijanje precizne geometrije različitih vrsta implantata, ono je primenjeno i u ovom istraživanju. Nakon detaljnog razvoja geometrije modela implantata kuka, koji podrazumeva 3D skeniranje i poboljšanja dobijenog oblaka tačaka do nivoa koji bi realno predstavljao stvarni implantat kuka, napravljeni su numerički modeli na osnovu dobijene geometrije. Rezultati ovih simulacija, sprovedenih metodom konačnih elemenata u softverskom paketu ANSYS<sup>®</sup> daju realne vrednosti napona u najkritičnijim oblastima veštačkog kuka. Tačna vrednost opterećenja pri kojem se javljaju plastične deformacije u implantu je određena i primenjena kao granični kriterijum za izbor opterećenja za dalje analize. Ove analize će obuhvatiti ocenu zamornog veka veštačkih kukova sa istom geometrijom i materijalom, u prisustvu prslina u najkritičnijoj oblasti.

for complex geometries, material properties, and specific boundary conditions. Consequently, the finite element method is considered a computational tool suitable for determining stresses and strains at any given point within a structure of arbitrary geometric and material complexity. The finite element model relies on an accurate constitutive representation of biomaterial properties, geometry data, loading properties, boundary conditions, and junction conditions. For example, three-dimensional models are most often used in orthopaedics, but in some cases, two-dimensional models can also be used for simplified analyses. FEM meshes in orthopaedic implants related to the bone geometry and prosthesis structure are increasingly made based on geometric data obtained by computer tomography (CT) imaging, /9-12/.

In order to perform finite element analyses in an effective and adequate manner, it is necessary to combine this method with other approaches which can provide reliable and representative models. One of the most common methods for obtaining the geometry which represents the basis for numerical models is 3D scanning and is applied in this research as well. An example of 3D scanning equipment can be seen in Fig. 1. Hence, research presented here combines numerical simulations performed using finite element method and reverse engineering, /13, 14/ (in the form of 3D scanning).

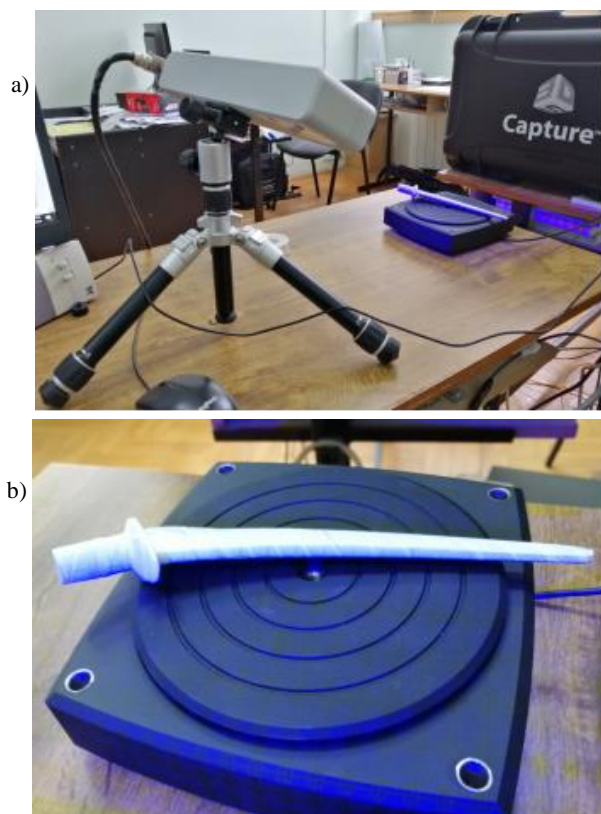


Figure 1. a) 3D scanner; b) support for scanned object, /15/.

#### APPLICATION OF REVERSE ENGINEERING IN BIOMEDICINE

The complex geometry of the human anatomy and the unique appearance of an individual human body have enabled greater utilization of scanning techniques in almost all medical fields. Scanning most often refers to the X-ray, CT, MRI, and ultrasound, for tissue and organ imaging purposes, /16/. Nowadays, conventional 3D scanning for outer surface/area imaging used in the industry (such as automotive, aerospace, etc.) has also been introduced in the medical field. Namely, such 3D scanners are an integral component in digital dentistry /17, 18/, and personalised medicine, /19, 20/. Usually, these 3D scanners use UV spectra as a light source. In digital dentistry two types of 3D scanners are used: intraoral and extraoral. Intraoral scanners are used for imaging dental arches, directly from a patient (Fig. 2a). Extraoral ones are used as an extra tool if there is only a conventional cast dental model available. In that case, imaging is conducted on a conventional cast model (Fig. 2b). Both 3D scanning types create a digital model as an output.

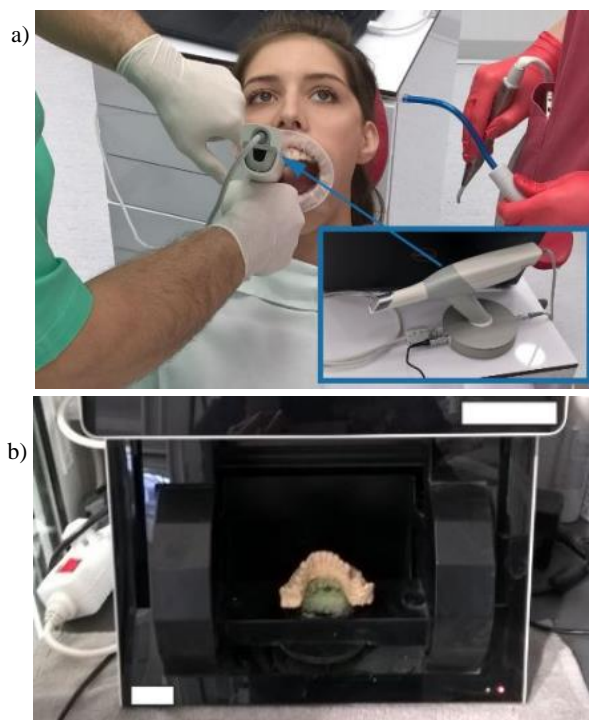


Figure 2. a) Dental arch imaging via intraoral scanner; b) dental model digitization via extraoral scanner.

#### REVERSE ENGINEERING OF A TITANIUM ALLOY HIP IMPLANT

Creating a representative CAD model is not an easy task and requires extra attention. Namely, obtaining such a model from a real specimen can be achieved by 3D scanning which often refers to reverse engineering. Using this approach, it is possible to graphically reconstruct an existing object. The graphic reconstruction then serves as the basis for the mesh of elements, and the automatic mesh generation (to some extent) is an advantage of this procedure. Despite other advantages and benefits of the non-destructive collection of geometric data, the problem of creating an adequate three-dimensional mesh remains. Numerical models of the partial hip prosthesis had to be made for the numerical analysis presented in this paper, to analyse the biomaterial behaviour in the implant during loading in the ideal case of walking and in the case of loads greater than expected.

In this sense, the problem of the placed prosthesis is simplified, hence, the required sizes could be monitored as realistically as possible. In the real case, many influencing factors affect the integrity of the prosthesis, such as the bone condition, the corrosion influence, and biocompatibility, but it is highly difficult to simulate all these factors since they depend on individual cases. For the FEM analysis, 3D models of the prosthesis are created based on real components of the prosthesis in the commercial software ANSYS R2.2022. For model preparation, the 3D scanning procedure is necessary to obtain the exact geometry of the prostheses. To successfully perform the analysis on various implant models with corresponding loads and to fulfil the goal of obtaining the stress state of the implant during loading, the necessity is to digitize the real models and translate them into a suitable form for computer recognition. Therefore,

the selected implants are scanned with an optical 3D scanner and recorded in STL (Standard Tessellation Language) format. Digitization of selected partial hip prostheses, extracted after revision from the human body, involved the use of modern equipment that provides output files that can be further processed into files compatible with the software used to repair the scanned models. For this purpose, two of the several samples of the partial hip prosthesis are chosen for scanning with the optical scanner.

Due to a certain error made by the scanner when recognizing the geometry, the obtained scanned models were not a completely faithful copy of the original. Additionally, the original '.stl' file is not suitable for defining the mesh of finite elements hence the output files are imported into the CAD software package which can both model the structure and save it in the appropriate file format. Within this package, the geometry has been repaired, refined, and prepared for export to FEM software.

As for the 3D scanning stage, the selected hip replacement implant was scanned on an Atos Core 200 3D scanner, a two-camera set device with a fixed turntable and scanning head (see Fig. 3). The measuring area here is 200×150 mm, with the model distance from the scanning head of circa 250 mm. The scanning resolution is set to 0.13 mm, sufficient for further CAD modelling. Before 3D scanning, a model is sprayed with white powder to enhance the contrast and is fixed to the turntable to enhance scanning precision. The scanning is performed at room temperature.



Figure 3. Atos Core 200 3D scanner setup, /31/.

The output of the 3D scanning is a cloud of points, also known in the field as 'mesh' (see Fig. 4a). Such mesh is preferred for CAD modelling of complex geometry models lacking 'blueprint' documentation. The procedure is commonly known as 'reverse engineering'. Hence, the resulting CAD model is shown in Fig. 4b.

The CAD modelling here is performed in SolidWorks® software (Dassault Systèmes, Vélizy-Villacoublay, France), with a dedicated add-in for such modelling procedure. Utilizing that add-in, the deviations of the created CAD model from the mesh can be assessed.

The output of deviation analysis is visualized in Fig. 5. The goal of the geometry optimisation process here is to decrease all deviations to a tolerable level. This includes both

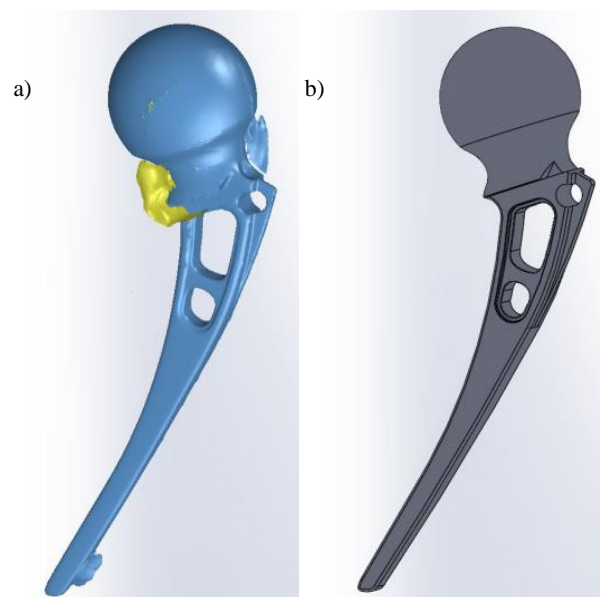


Figure 4. a) Chosen hip replacement implant model's point cloud (mesh); b) Created and optimised CAD model.

the missing parts of the model, such as holes (negative deviations), and the excess parts of the model, i.e., portions of geometry that do not exist in the actual scanned hip implant (positive deviations). The maximal deviations in Fig. 5 are not greater than 1 mm, thus proving the adequacy of the created CAD model and providing a solid basis for the next stage - the development of numerical models. The final version of the model is exported as a STEP (Standard for the Exchange of Product data) file- used in various types of FEM software.

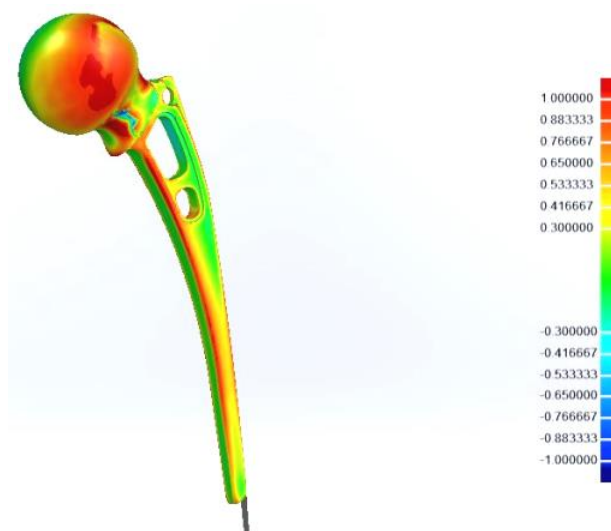


Figure 5. Deviation analysis of CAD model from dedicated mesh.

## DEVELOPMENT OF NUMERICAL MODELS

This section of the paper describes the process of developing the numerical models used in static calculations in detail. The finite element method is chosen based on several factors: efficiency and reliability in simulating a wide range of different engineering problems, applicability to numerous scientific and industrial fields, and the previous good experience of the paper's authors. The finite element method in

this case is used due to the ability to provide quick insight into the stress state of a structure subjected to static loads, once boundary conditions, loads, and the finite element mesh are all adequately defined and adopted. Another advantage of this method is the ability to simulate fatigue crack growth in various structures which will represent the following steps in this extensive research, related to the structural integrity of hip implants with optimised geometry.

The first step was the creation of hip implant geometry, which was achieved via 3D scanning as explained in the previous chapters, so that it could be imported into the ANSYS SpaceClaim module, Fig. 6. The next step involved running numerical simulations for different load cases, including walking, climbing up and down stairs, tripping, etc. All of these cases were considered for a person weighing 90 kg. The main aim of these simulations was to verify the 3D-scanned model for further simulations. In addition, these models could help determine which load cases could be considered for fatigue crack growth analysis, by providing information concerning the hip implant's most critical location in terms of stress, thus defining the most probable location of fatigue crack initiation.

The next step was to define the material properties needed for the calculations - with the most important parameters being the yield stress and tensile strength of the utilized Ti-6Al-4V alloy. This data was obtained from previously per

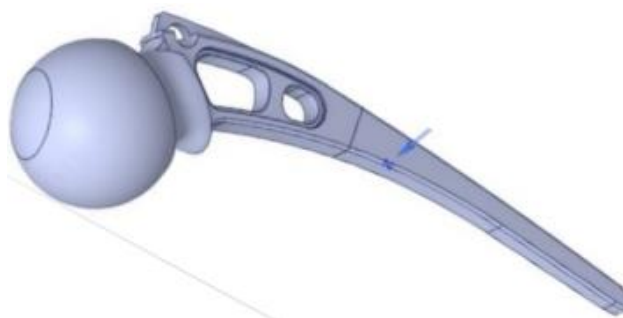


Figure 6. Geometry of the numerical model of the hip implant from ANSYS, based on the imported 3D scan.

formed experiments involving hip implants, which can be found in [21, 22]. These material properties, along with others required for static calculation in ANSYS, are shown in Fig. 7. The most important material properties in this case included Young's modulus, Poisson's ratio, yield strength and ultimate tensile strength. Since one of the goals of these finite element method simulations was to determine which load cases will cause the hip implant to enter plasticity, the plastic behaviour needed to be defined as well. It was included in the form of a bilinear isotropic hardening, with corresponding parameters - yield stress which was the same as in the case of elastic parameters, and tangent modulus, determined based on ultimate tensile strength.

Properties of Outline Row 3: Ti-6Al-4V			
	A	B	C
	Property	Value	Unit
1			
2	Material Field Variables	Table	
3	Isotropic Elasticity		
4	Derive from	Young's Modulus and Poisson...	
5	Young's Modulus	1.1E+05	MPa
6	Poisson's Ratio	0.3	
7	Bulk Modulus	91667	MPa
8	Shear Modulus	42308	MPa
9	Bilinear Isotropic Hardening		
10	Active Table	Plastic	
11	Yield Strength	780	MPa
12	Tangent Modulus	1358	MPa
13	Tensile Yield Strength	780	MPa
14	Tensile Ultimate Strength	860	MPa

Figure 7. Material properties of Ti-6Al-4V alloy used in the numerical simulations.

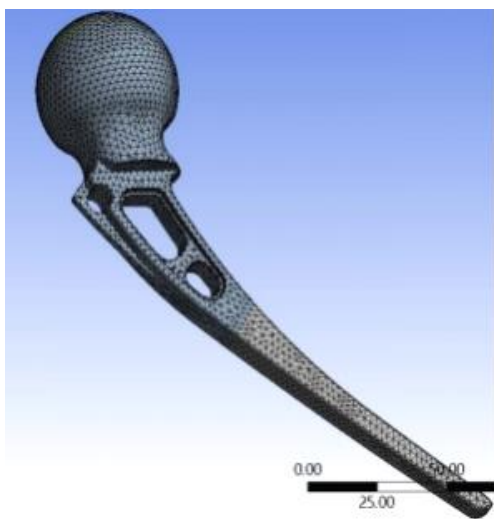


Figure 8. Finite element mesh of the hip implant model.

Once the material was properly defined and the geometry successfully imported, the next step involved defining loads and boundary conditions, along with the generation of the finite element mesh. Due to the geometry of the orthopaedic hip implant and the fact that these models would be later used as a base for fatigue simulations, tetrahedral elements are adopted. The generated finite element mesh is shown in Fig. 8. Several different finite element sizes were tested, in order to ensure proper result convergence, as is common practice in finite element modelling. Figure 9 shows the final mesh, for which it was determined that it provides the most accurate results. The load is defined as a concentrated force acting in the implant head, corresponding to how the load is applied during the experiment. An example of the load can be seen in Fig. 9. Boundary conditions are simply defined as fixed in the bottom half of the model. As previously mentioned, a total of four different load cases are assumed.

Load magnitudes are calculated by multiplying the selected weight with appropriate coefficients and converting into Newtons. Obtained loads were as follows:

- walking - 2490 N,
- climbing downstairs - 3143 N,
- climbing upstairs - 3417 N,
- tripping - 6358 N.

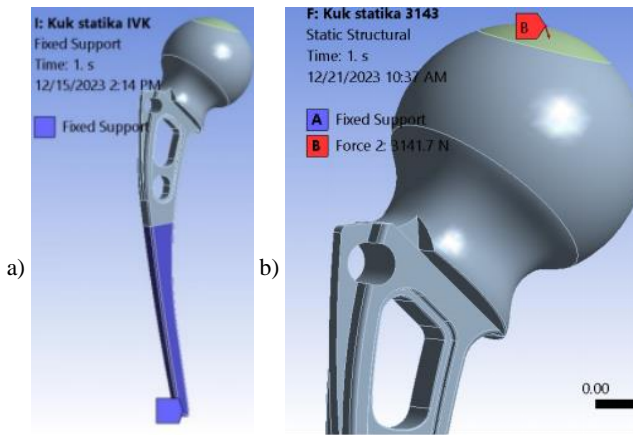
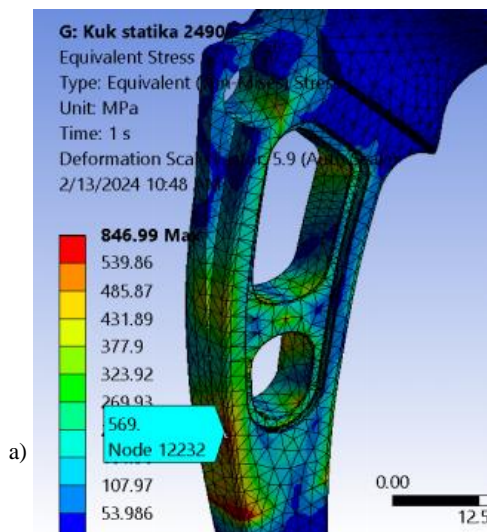
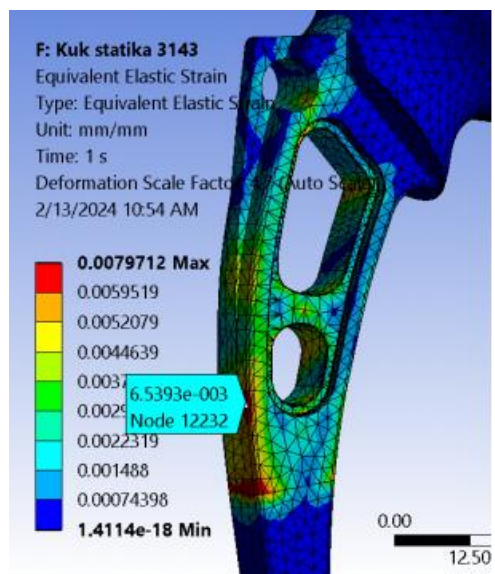
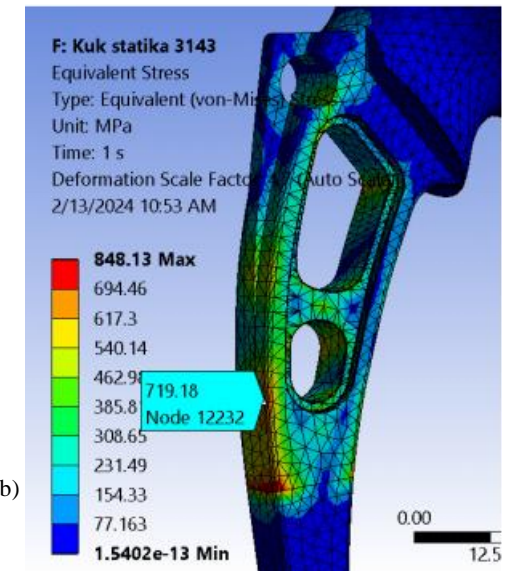
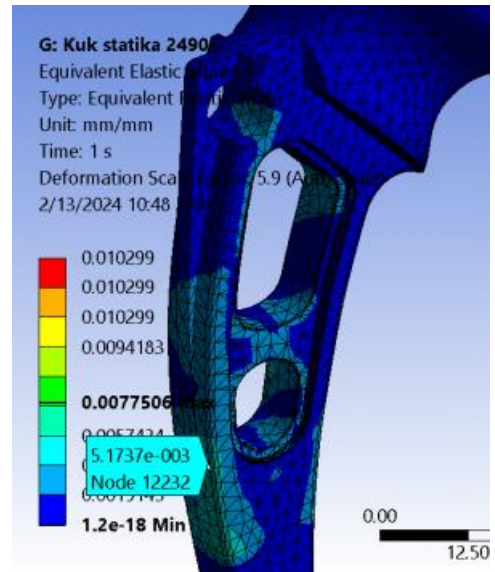


Figure 9. a) Boundary conditions for all models; and b) load in the form of a concentrated force for one of the cases.

RESULTS AND DISCUSSION

Results for stresses and strains in four load cases are shown in Fig. 10. The focus is on the location of the highest tensile stress which in all presented cases occurred in the same location. This critical location corresponds to the location in the test specimens where failure was initiated, /22/, confirming the validity of the simulations. Strain values in Fig. 10 correspond to these critical stress locations as well. To avoid confusion, it should be noted that the highest strain is observed in the area of the implant head where the concentrated force is applied, but these values can be dismissed. In some cases, deformation in this region is so high that it enters plasticity, while the rest of the hip model remains in the elastic area. For similar reasons, stress values near the boundary conditions are also neglected, as their presence is a direct consequence of constraints in that area. More details on why these stresses are not realistic can be found in /23/.



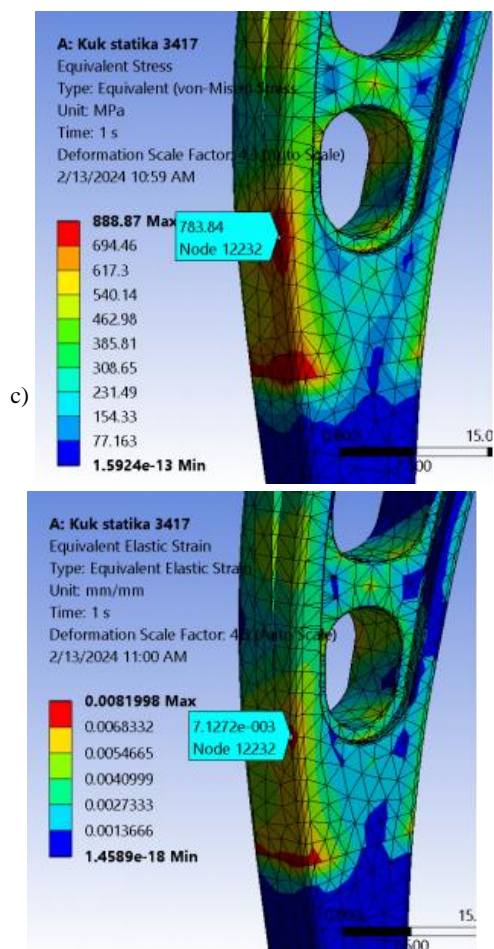


Figure 10. Stress distribution for all load cases: a) first load case, 2490 N force; b) second load case, 3143 N force; c) third load case, 3417 N force.

For the first two cases, with forces of 2940 N and 3143 N, respectively, the highest tensile stresses did not exceed the yield stress of the alloy (780 MPa), thus remaining in the elastic zone. Maximal tensile stresses reached here are 569 and 719 MPa, respectively. The corresponding strains were 0.51 % for the 2940 N load case, and 0.65 % for the second case, 3143 N.

Interestingly enough, in the third case, the load 3417 N resulted in a maximal tensile stress of 783 MPa, which is near the yield stress level for the used titanium alloy, as defined in the material properties. This implies that the load case that introduces plasticity is the third, and that any analyses beyond this point would only produce higher plastic strain, not only in the afore-mentioned hip implant head but in the critical area of the stem. This critical area, for all cases, is located on the outer side of the stem, in the vicinity of the lower, smaller opening - as expected, since the load-bearing cross-section area of the stem in this location is decreased due to the presence of the opening, and also due to the direction in which the load acts on the hip implant head.

Since the plasticity limit of the numerical hip implant model was reached with the third load case, there was no need to run the final simulation, since a much higher load (6853 N) would result in considerable plastic strain and is not of interest in terms of fatigue behaviour, which will be the main focus of the continuation of the work presented here.

## CONCLUSION

In this paper, a reverse engineering methodology relying on 3D scanning of real orthopaedic hip implants is combined with the finite element method to analyse the behaviour of such implants under various load cases. Obtaining a representative CAD model from 3D scanning, however, was not a simple process, as certain adjustments needed to be made to the scanned geometry to ensure it resembles the real hip implant as much as possible.

Having in mind that these results are presented for normal body weight (90 kg), it can be concluded that an increase in body weight represents a potential problem even at static loading, for this specific geometry. The material of choice, Ti-6Al-4V, is very sensitive to notches, hence these loading conditions, combined with implant geometry, could lead to failure.

Finally, it can be seen that the results obtained by this research indicate the following:

- climbing upstairs can cause plastic strain for the given geometry of the implant, for a body weight of 90 kg,
- hence, fatigue analysis in this case would only make sense for the first two loads (out of four considered possibilities).
- Numerical models have shown expected results, suggesting that the reverse engineering method applied to obtain accurate geometry of hip implants was performed adequately,
- this particular optimised hip implant geometry which included two holes in the stem, is not an ideal solution for the selected body weight, due to plastic strain occurring even under static load in certain cases.

An additional contribution of this research is reflected in the results of the third case model (force of 3417 N) which represents the moment at which the model enters plasticity. This suggests that the existing models can also be used to determine such critical loads iteratively, while obtaining sufficiently accurate results in a very efficient manner, since the only parameters that need to be varied are the loads, thus calculations can be done quickly.

The final outcome of this research is obtaining of a solid, reliable base for future work through a combination of reverse engineering and finite element analysis.

## ACKNOWLEDGEMENT

The authors of this paper would like to express their gratitude to the Ministry of Science, Technological Development and Innovations, of the Republic of Serbia for their help and support through contracts 451-03-68/2022-14/200105 and 451-03-68/2022-14/200135.

## REFERENCES

1. Heller, M.O., *Chapter 32 - Finite element analysis in orthopedic biomechanics*, In: B. Innocenti, F. Galbusera (Eds.), *Human Orthopaedic Biomechanics: Fundamentals, Devices and Applications*, Academic Press, Elsevier, pp. 637-658, 2022. doi: 10.1016/B978-0-12-824481-4.00026-3
2. Bori, E., Innocenti, B. (2023), *Biomechanical analysis of femoral stem features in hinged revision TKA with valgus or varus deformity: A comparative finite elements study*, *Appl. Sci.* 13(4): 2738. doi: 10.3390/app13042738

3. Yan, L., Lim, J.L., Lee, J.W., et al. (2020), *Finite element analysis of bone and implant stresses for customized 3D-printed orthopaedic implants in fracture fixation*, Med. Biol. Eng. Comput. 58(5): 921-931. doi: 10.1007/s11517-019-02104-9
4. Khalaf, K., Azhang, A., Cheng, C-H, Nikkhoo, M. (2023), *Bio-mechanical investigation of bone screw head design for extracting stripped screw heads: Integration of mechanical tests and finite element analyses*, Materials, 16(15): 5470. doi: 10.3390/ma16155470
5. Kladovasilakis, N., Tsongas, K., Tzetzis, D. (2020), *Finite element analysis of orthopedic hip implant with functionally graded bioinspired lattice structures*, Biomimetics, 5(3): 44. doi: 10.3390/biomimetics5030044
6. Falcinelli, C., Valente, F., Vasta, M., Traini, T. (2023), *Finite element analysis in implant dentistry: State of the art and future directions*, Dental Mater. 39(6): 539-556. doi: 10.1016/j.dental.2023.04.002
7. Gerasimov, O.V., Kharin, N.V., Fedyanin, A.O., et al. (2021), *Bone stress-strain state evaluation using CT based FEM*, Front. Mech. Eng. 7: 688474. doi: 10.3389/fmech.2021.688474
8. Xie, W., Lu, H., Zhan, S., et al. (2022), *Establishment of a finite element model and stress analysis of intra-articular impacted fragments in posterior malleolar fractures*, J Orthop. Surg. Res. 17: 186. doi: 10.1186/s13018-022-03043-2
9. Guha, I., Zhang, X., Rajapakse, C.S., et al. (2022), *Finite element analysis of trabecular bone microstructure using CT imaging and continuum mechanical modeling*, Med. Phys. 49(6): 3886-3899. doi: 10.1002/mp.15629
10. Benca, E., Amini, M., Pahr, D.H. (2020), *Effect of CT imaging on the accuracy of the finite element modelling in bone*, Eur. Radiol. Exp. 4: 51. doi: 10.1186/s41747-020-00180-3
11. Rayudu, N.M., Dieckmeyer, M., Löffler, M.T., et al. (2021), *Predicting vertebral bone strength using finite element analysis for opportunistic osteoporosis screening in routine multidetector computed tomography scans-A feasibility study*, Front. Endocrinol. 11: 526332. doi: 10.3389/fendo.2020.526332
12. Sollmann, N., Rayudu, N.M., Lim, J.J.S., et al. (2021), *Multi-detector computed tomography (MDCT) imaging: association of bone texture parameters with finite element analysis (FEA)-based failure load of single vertebrae and functional spinal units*, Quant. Imaging Med. Surg. 11(7): 2955-2967. doi: 10.21037/qims-20-1156
13. Santoši, Ž., Budak, I., Šokac, M., Pavletić, D. (2019), *Bridging the symmetry-related gap between physical and digital sculpting by application of reverse engineering modelling*, FME Trans. 47(2): 304-309. doi: 10.5937/fmet1902304S
14. Pathak, V.M., Srivastava, A.K., Gupta, S. (2020), *Methodology for GD&T verification in an innovative benchmark part for contactless scanning systems*, FME Trans. 48(4): 899-907. doi: 10.5937/fme2004899K
15. Mijatović, T., Milovanović, A., Sedmak, A., et al. (2019), *Integrity assessment of reverse engineered Ti-6Al-4V ELI total hip replacement implant*, Struct. Integr. Life, 19(3): 237-242.
16. Haleem, A., Javaid, M. (2019), *3D scanning applications in medical field: A literature-based review*, Clin. Epidem. Global Health, 7(2): 199-210. doi: 10.1016/j.cegh.2018.05.006
17. Javaid, M., Haleem, A., Kumar, L. (2019), *Current status and applications of 3D scanning in dentistry*, Clin. Epidem. Global Health, 7(2): 228-233. doi: 10.1016/j.cegh.2018.07.005
18. Sehrawat, S., Kumar, A., Grover, S., et al. (2022), *Study of 3D scanning technologies and scanners in orthodontics*, Mater. Today: Proc. 56 (Part 1): 186-193. doi: 10.1016/j.matpr.2022.01.064
19. Lazzeri, S., Talanti, E., Basciano, S., et al. (2022), *3D-Printed patient-specific casts for the distal radius in children: outcome and pre-market survey*, Materials, 15(8): 2863. doi: 10.3390/ma15082863
20. Farhan, M., Wang, J.Z., Bray, P., et al. (2021), *Comparison of 3D scanning versus traditional methods of capturing foot and ankle morphology for the fabrication of orthoses: a systematic review*, J Foot Ankle Res. 14(1): 2. doi: 10.1186/s13047-020-00442-8
21. Sedmak, A., Čolić, K., Grbović, A., et al. (2019), *Numerical analysis of fatigue crack growth of hip implant*, Eng. Fract. Mech. 216: 106492. doi: 10.1016/j.engfracmech.2019.106492
22. Colic, K., Sedmak, A., Grbovic, A., et al. (2016), *Finite element modeling of hip implant static loading*, Procedia Eng. 149: 257-262. doi: 10.1016/j.proeng.2016.06.664
23. Čolić, K., Sedmak, S., Sedmak, A., et al. (2024), *Numerical analysis of static stresses in partial hip implant*, Struct. Integr. Life, 24(1): 17-20.

© 2024 The Author. Structural Integrity and Life, Published by DIVK (The Society for Structural Integrity and Life 'Prof. Dr Stojan Sedmak') (<http://divk.inovacionicentar.rs/ivk/home.html>). This is an open access article distributed under the terms and conditions of the [Creative Commons Attribution-NonCommercial-NoDerivatives 4.0 International License](#)